Structural and Optical Properties of Doped Polystyrene Thin Films by (NiO, TiO₂, ZnO, MgO) Nanoparticles

H. K. AL-Rubaiawi[1], A. Faisal Alwan[2], A. Ayad Husain[*2], N. Muhamed Ibrahim[2], D. Abdul Kareem Ali[1], A. Tariq Mahmood[2]

[1.] Chemistry Department, College of Science, Mustansiriyah University, P.O. Box: 14022, Baghdad, Iraq

[2.] Polymer Research Unit, College of Science, Mustansiriyah University, P.O. Box: 14022, Baghdad, Iraq

ABSTRACT

*T*his study aims to fabricate polystyrene-based nanocomposite thin films with improved optical, dielectric, and photostability properties to address challenges in optoelectronic and photonic applications, especially in extreme environments. The casting process included the incorporation of doped nanoparticles, specifically ZnO, TiO₂, NiO, and MgO, into polystyrene. Thin films were produced with a consistent concentration of 5 g of polystyrene, incorporating 0.01 g of different nanomaterials. UV-Visible spectroscopy was employed to analyze the samples across a wavelength range of 200-1100 nm, assessing oscillator strength, optoelectronic properties, and optical characteristics. All nanocomposite films demonstrated enhanced reflectance and transmittance, alongside improved optoelectronic properties, such as high-frequency dielectric performance and effective mass. These films improve photostability in the presence of UV radiation and harsh environmental conditions, rendering them appropriate for undersea, aeronautical, and aerial transport applications. They also provide potential for UV radiation shielding and have applications in light-emitting diodes, laser sensors, memory devices, and light-harvesting systems. Prog. Color Colorants Coat. 18 (2025), 323-341© Institute for Color Science and Technology.

1. Introduction

Intercalated polymer nanocomposites (NCs) containing nanometal oxides are gaining popularity in academic and industrial environments. The technique involves selecting polymers and metal oxides at the nanoscale from a diverse array of available polymers and nanomaterials to get specific desired characteristics. Metal oxides are widely recognised for their versatility and are used in various applications, including sensors, photocatalytic systems, fuel cells, coatings, and optoelectronic devices [1, 2]. The surface properties of metal oxides play a crucial role in determining the efficiency of their interactions with target molecules. Reducing the size of metal oxide particles to the nanoscale increases the surface area available for chemical reactions, giving rise to a phenomenon known as quantum confinement [3]. characterized by an elevated energy band gap, enhanced ultraviolet (UV) absorption, room-temperature activity, and light emission upon excitation-well-documented in previous studies. Compared to conventional spherical nano metal oxides, these nanoscale materials exhibit superior electrical properties and distinct morphologies that can significantly improve the conductivity of industrial polymers, which is particularly beneficial for the electronics industry, relying heavily on components like resistors, inductors, and capacitors [4].

The surface chemistry of nanometal oxides includes

unoccupied orbitals that facilitate charge transfer with host polymers. The properties of polymeric nanocomposites are influenced by factors such as component composition, structural arrangement, the quantity and morphology of incorporated nanometal oxides, and interfacial interactions within the composite matrix. Optimizing these interactions is crucial for enhancing the optoelectronic properties of polymeric nanocomposites. Integrating inorganic nanoparticles can substantially improve the physical and optical properties of polymers. Polymeric/inorganic nanocomposites [2] offer a synergistic blend of both components' advantageous properties-polymers provide mechanical robustness and flexibility, while inorganic nanomaterials enhance optical and electrical characteristics [5].

Polystyrene (PS), a widely used thermoplastic polymer, is favored for its transparency, resistance to diluted acids and bases, cost-effectiveness, and manufacturability. It has numerous applications across various industries, including disposable consumer goods and optical, electronic, and medical components. Its optical properties make it ideal for optoelectronic applications, and incorporating nanometal oxide particles can significantly enhance its optical, structural, and electronic characteristics. For example, titanium dioxide (TiO_2) improves UV radiation resistance while increasing opacity and brightness, zinc oxide (ZnO) offers UV shielding and antibacterial properties, and nickel oxide (NiO) can modify PS's optical bandgap for applications such as UV protection, photovoltaics, and sensors. NiO also enhances the refractive index of PS, improving performance in optical systems requiring precise light manipulation [6, 7]. Additionally, magnesium oxide (MgO) provides excellent transparency in the UV-Visible spectrum, enhancing optical clarity and UV protection, particularly beneficial for coatings and packaging. MgO also boosts PS's photoluminescent properties, making it valuable for light-emitting diode (LED) applications [8-10].

This study explores the fabrication of polystyrene (PS) nanocomposite thin films incorporating various metal oxide nanoparticles, including ZnO, TiO_2, NiO, and MgO. Unlike previous research, this work provides a thorough analysis of how each nanoparticle type influences key material properties. A comprehensive evaluation of optical and structural properties aims to enhance dielectric performance, photostability, and overall optoelectronic efficiency, making these nanocomposites highly suitable for advanced photonic and optoelectronic applications like UV shielding, LEDs, and sensor technologies, especially under extreme environmental conditions [11].

2. Experimental

2.1. Materials

Polystyrene, ethanol, and chloroform with 99 % purity were acquired from PetKim Petrokimya, located in Istanbul, Turkey. All nano oxides were obtained from Hunan/ Changsha Easchem in China. These nano-particles had 99 % purity.

2.2. Testing devices

The synthesized, altered, and doped polymer was evaluated by the ultraviolet and visible spectra of films, recorded using a SHIMADZU UV-1800 Spectro-photometer, which measured the transmittance and absorbance spectrum within the 200-1100 nm range. This spectrometer incorporates two light sources: a Deuterium lamp for the wavelength range of 190-390 nm and a Tungsten lamp for the range of 390-1100 nm. The output statistics of wavelength reflectance, transmittance, and absorbance are used in a computer program to ascertain all optical constants. The morphological characterization of PS nanocomposite films was measured using the SEM (scanning electron microscope) (15.0 kV SE). AFM (atomic force microscopy) (Mountains SPIS Academic 10.0.10483) was used to quantify the surface roughness of the PS nanocomposite.

2.3. Blank PS thin film fabrication

To produce the blank thin film, 1 g of commercial PS was dissolved in 100 mL of chloroform. The solution was homogenized by mechanically agitating it using an ultrasonic device for three hours. Then, a film with a thickness of 40 Mm was obtained by pouring a PS solution over a glass plate. Next, the film was covered and left to dry for about 45 hours at ambient temperature.

2.4. Preparation of PS/nano oxide

1 g of commercial PS was dissolved in 100 mL of chloroform to generate the blank thin film. The solution was mechanically agitated for three hours using an ultrasonic device to achieve homogeneity. The PS solution was poured over a glass plate, forming a 40

μm-thick film. Next, the film was covered and allowed to dry at ambient temperature for approximately 45 hours [12].

3. Results and Discussion

3.1. Fourier transform infrared spectroscopy (FTIR) analysis for polystyrene (PS)

The reaction was analyzed using Fourier Transform Infrared Spectroscopy (FTIR) for the PS, as seen in Figure 1, which displays the FTIR data of the absorption peaks of the PS thin film. The results indicate that absorption peaks occurred for the aromatic C-H stretch between 3000 and 3100 cm^{-1} and the aromatic C=C stretch at around 1600 and 1490 cm^{-1}. The peaks at 1450 cm^{-1} and 1370 cm^{-1} indicate bending vibrations.

3.2. PS and PS/ nano-oxides films reflection test

PS and PS nano oxides thin films with various nanoparticles show an increase in reflectance (R) from 0.2 for both blank PS and PS nanocomposite thin films, as illustrated in Figure 2. This reflectance continues to rise until it stabilizes at wavelengths of λ ≥ 500 nm. Nanoparticles influence wavelength-dependent reflectance, selectively reflecting certain light wavelengths more than others. MgO exhibits the highest UV reflectance due to its transparency, while ZnO enhances reflectance in both UV and visible ranges due to strong UV absorption. TiO₂ significantly increases visible reflectance, and NiO contributes moderately. These improvements result from the high refractive indices of the nanoparticles, which effectively scatter

and reflect light. Additionally, the quantum confinement effect and surface plasmon resonance in nanoparticles like ZnO and TiO₂ enhance selective wavelength reflectance. The incorporation of MgO, ZnO, TiO₂, and NiO into polystyrene can enhance reflectance, as each nanoparticle offers unique optical properties. These characteristics enable the creation of materials with tailored reflectance suitable for applications ranging from reflective coatings to optical devices.

3.3. Absorption coefficient of PS and PS/nano oxide films

The metal Oxide Nanoparticles added to polystyrene are well-known for their strong UV absorption capabilities. When these nanoparticles are added to polystyrene, they increase the material's absorption coefficient in the UV region. This is due to their wide bandgap and strong interaction with UV light, which allows them to absorb and dissipate UV radiation effectively [12, 13]. The absorption spectra of PS thin films are calculated from the equation 1 [14]

$$\alpha = 2.303 \times \frac{A}{t} \qquad (1)$$

Where α is the absorbance coefficient in cm^{-1}, A is absorbance, and t is the coating thickness. This equation, based on the Beer-Lambert law, relates absorbance, film thickness, and absorption coefficient. It is particularly suitable for analyzing thin films, as it accurately quantifies the amount of light absorbed per unit thickness. This information is crucial for evaluating the optical properties of nanocomposite materials.
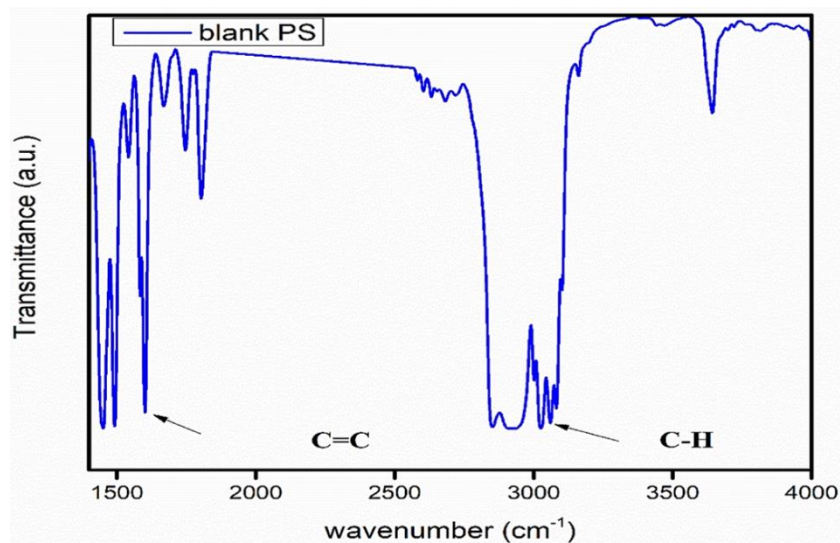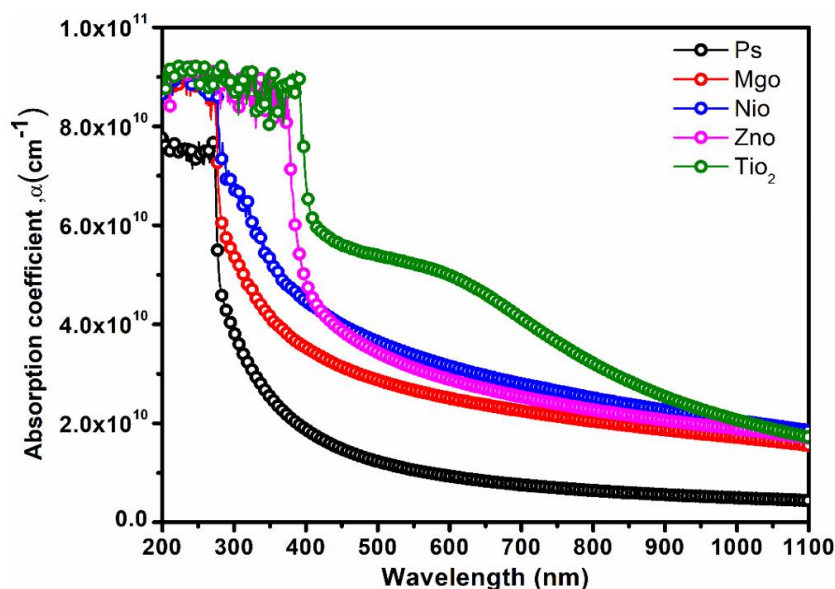

Figure 1: FTIR spectra for polystyrene PS.

Figure 2: Absorption coefficient of blank PS, and PS/nano oxide films.

Figure 2 illustrates that within the wavelength range of 500 nm to 1000 nm, which spans the transition from visible light to near-infrared, polystyrene exhibits a low absorption coefficient in the ultraviolet (UV) region due to its bandgap. However, doping polystyrene with nanoparticles such as TiO_2, ZnO, NiO, or MgO significantly enhances its UV absorption. Notably, absorption tends to decrease in the UV region (below 400 nm) because the lower photon energy makes electronic transitions in these materials less likely to occur.

Among the doped nanoparticles, TiO_2 stands out for having the highest UV absorption, particularly below 400 nm, attributed to its strong photocatalytic activity and high refractive index. ZnO also shows strong UV absorption due to the effective interaction of its wide bandgap with UV light. NiO displays moderate UV absorption, which is influenced by its bandgap and surface interactions. In contrast, MgO demonstrates the lowest absorption among the nanoparticles because of its high transparency and low absorption coefficient. The optimal sample is the nano oxide thin film (PS/TiO_2), which exhibits a superior absorption coefficient compared to the other samples [15, 16].

3.4. Transmittance of PS and PS/nano oxide films

The inclusion of nanoparticles into polystyrene often leads to a decrease in transmittance, particularly in the ultraviolet (UV) spectrum, due to increased absorption and scattering of light. The extent to which this decrease occurs depends on the particular attributes of the nanoparticles, such as their kind, dimensions, concentration, and spatial arrangement [17]. Meticulously engineered nanocomposites may maintain a significant degree of light transmission within the visible spectrum while effectively blocking ultraviolet (UV) radiation. This characteristic renders them very advantageous in many optical applications [18]. They are also used in windows, eyeglasses, and coatings designed to protect against UV radiation. Furthermore, in applications such as screens, ensuring a high level of transmittance in the visible spectrum while effectively filtering UV or other undesired light may enhance both performance and longevity. Figure 3 demonstrates that the optimum sample is the nanocomposite thin film (PS/TiO_2), which displays a reduced transmittance (T) value relative to the blank PS and PS with alternative nanoparticles [19].

3.5. Skin depth of PS and PS/nano oxide films

These nanoparticles are renowned for their high specific absorption in certain areas of the electromagnetic spectrum, especially in the ultraviolet (UV) region. When these nanoparticles are incorporated into polystyrene, they enhance the overall absorption of the material. Hence, the skin depth decreases due to the faster attenuation of the electromagnetic wave inside the material [20]. Superb absorption leads to decreased skin depth. Incorporating nanoparticles into polystyrene substantially reduces
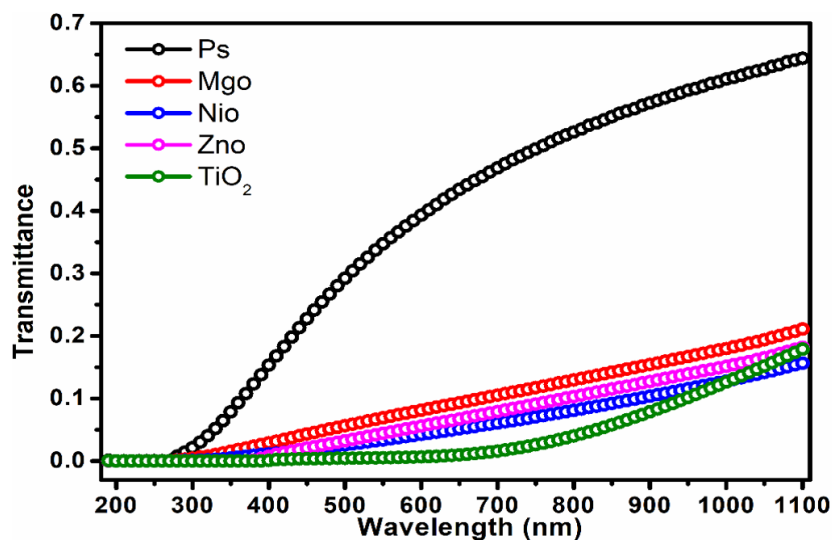
Figure 3: Transmittance of blank PS, and PS/nanoparticle films.

the skin depth in the ultraviolet (UV) region due to these materials' efficient absorption of that particular light spectrum. High refractive index nanoparticles, such as TiO₂, induce enhanced reflection and absorption, decreasing skin depth, as demonstrated in (Figure 4). Consequently, the composite material exhibits increased opacity and reduced light penetration, particularly at shorter wavelengths. In contrast, the low refractive index nanoparticles have a much-reduced effect on the depth of the skin, particularly in the visible spectrum. Regulating skin depth is of utmost importance within

optical devices, whether to selectively filter certain wavelengths or develop sensors with accurate depth sensitivity. hence, the skin depth is determined by equation 2 [21-23].

$$x = \frac{\lambda}{2\pi k} \qquad (2)$$

Let x represent the skin depth in nanometers, λ represent the wavelength in nanometers and k represent the extinction factor.
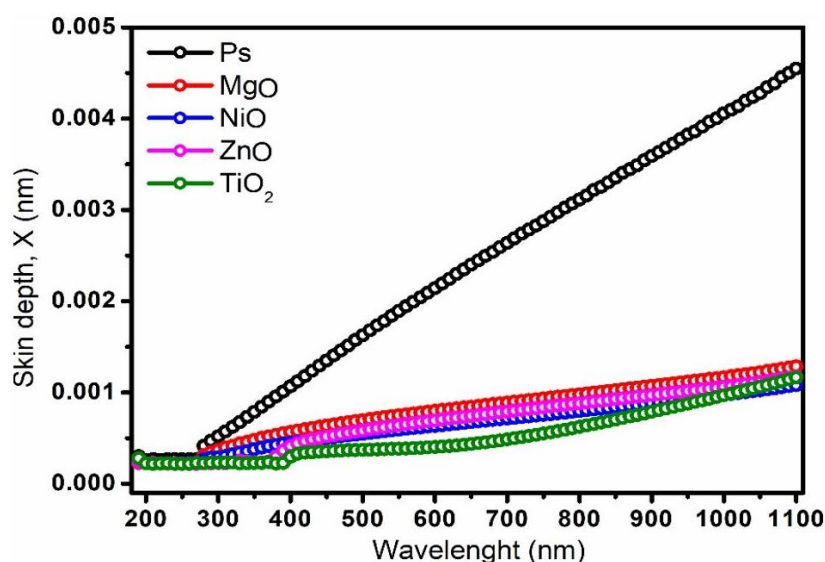

Figure 4: Skin depth of blank PS, and PS/nanoparticle films.

3.6. Refractive of PS and PS/nano oxide films

The incorporation of nano-oxides into polystyrene may markedly modify its refractive index. The refractive index of a substance quantifies the extent to which it refracts light during transmission. The dispersion of nano-oxides in a polymer matrix, such as polystyrene, influences the refractive index due to several variables, including material properties. Structure Nano-oxides often possess a superior refractive index compared to the polymer matrix [24]. Incorporating nano-oxides often elevates the composite material's total refractive index, contingent upon the quantity and kind of oxide used.

An increased concentration of nano-oxides will raise the polystyrene-nano-oxide composite's refractive index. Nonetheless, the connection is not always linear, particularly if the nano-oxides begin to congregate or engage with the polymer in intricate ways [25]. Moreover, the dimensions and even distribution of nano-oxides may affect the interaction of light with the composite. Well-dispersed nanoparticles may augment the refractive index more efficiently, but aggregation may induce light scattering, diminishing transparency and impacting the overall refractive characteristics.

The refractive index of polystyrene rises with the addition of nano-oxides, with the degree of variation influenced by the kind, concentration, size, and dispersion of the nano-oxides [26, 27]. As a result, the refractive index is determined from equation 3 where (n) denotes the refractive index, (R) represents reflectance, and (k) signifies the extinction factor [28].

$$n= \left[\frac{1+R}{1-R}\right] + \sqrt{\frac{4R}{(1-R)^2} - k^2} \tag{3}$$

The refractive index (n) initially demonstrates elevated values within the 300-700 nm wavelength range. This phenomenon results from the resonance effect of electromagnetic radiation interacting with the electrical polarization of electrons in the nanocomposite thin film structure, which is caused by the oscillation of the electric field. Subsequently, the refractive index stabilizes within the 700 nm wavelength range ($\lambda < 700$ nm), as illustrated in Figure 5.

3.7. Extinction factor of PS and PS/nano oxide films

Incoming wavelengths may absorb some light upon interacting with the particles on the thin film surface. The remainder is reflected off the particle surface, depending on the angle of incidence relative to the wavelength of light. The parameter representing absorbance losses is the extinction coefficient (k), as shown in Figure 6. It denotes the attenuation of electromagnetic waves travelling through the thin layers and is calculated using equation 4 [29, 30].

$$k = \frac{\alpha\lambda}{4\pi} \tag{4}$$

Where α is the absorption coefficient (cm^{-1}) and λ is the wavelength (nm). As a result, Figure 7 illustrates the extinction factor k for all samples, including the plain PS and PS thin films containing a variety of nanoparticles.
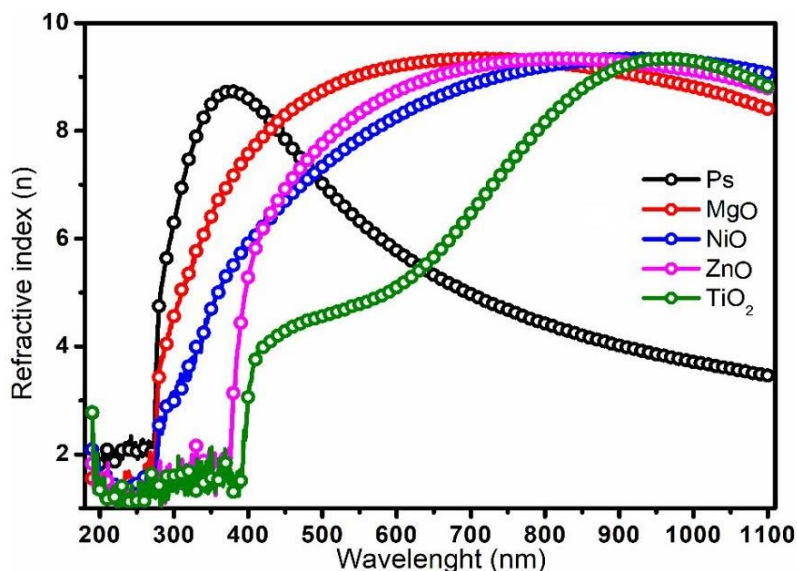

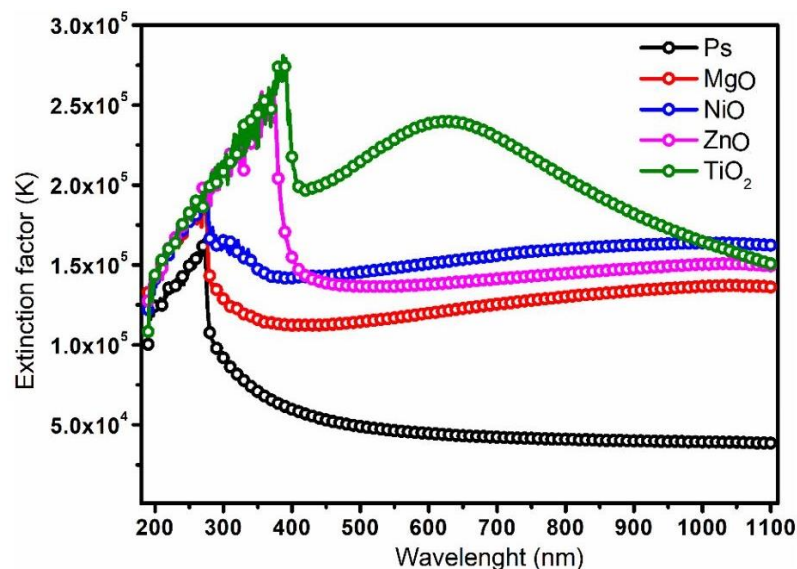**Figure 5:** Reflective index of blank PS and PS/nanoparticle films.

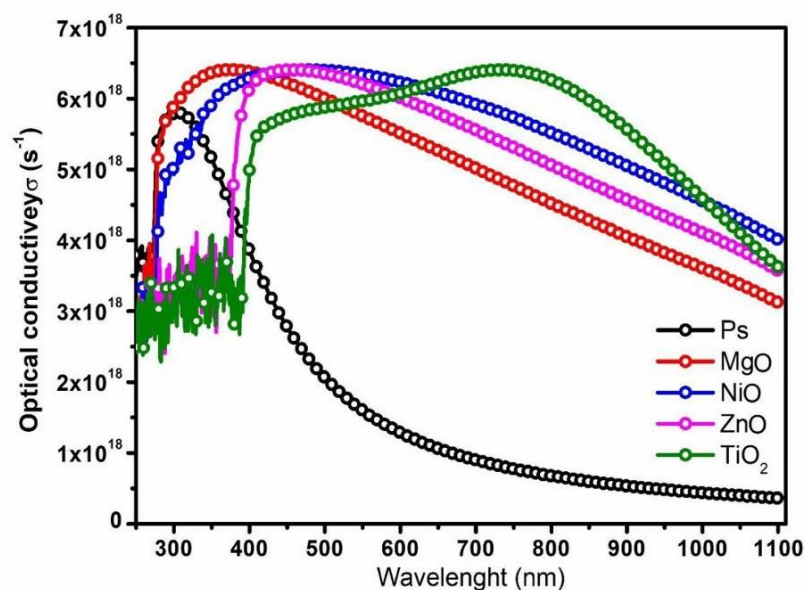**Figure 6:** Extinction factor (k) of blank PS, and PS/nano oxide films.

Figure 7: Optical conductivity (σ) of blank PS, and PS/nano oxide films.

Titanium dioxide (TiO$_2$) and zinc oxide (ZnO) are nano-oxides that exhibit substantial absorption in specific wavelength ranges, particularly within the ultraviolet (UV) spectrum. This absorption immediately improves the extinction coefficient in the ultraviolet spectrum. For example, the extinction coefficient of polystyrene would be improved throughout this range by incorporating TiO$_2$, which exhibits substantial absorption in the UV spectrum (200-400 nm). Additionally, ZnO exhibits exceptional UV radiation absorption [31].

In the visible spectrum, some oxides may demonstrate reduced absorption, contingent upon their size and crystalline structure, resulting in a negligible rise in the extinction factor. The interaction between the nano-oxides and the polystyrene matrix may alter the extinction factor. If the nanoparticles' surface is inadequately connected with the polymer, it may result in spaces and flaws, augmenting scattering and, consequently, the extinction factor [32, 33].

3.8. Optical conductivity of blank PS, and PS/ nano oxide films

The thin layer's conductance is provided by the optical conductivity (σ), which quantifies electron movement via band levels, when a portion of the incoming light is absorbed. The electron rapidly transitions between orbits, resulting in a vacancy in the valence band that improves the conductivity of the thin layer Figure 7 shows the optical conductivity (σ) of blank PS, and PS/nano oxide films. Equation 5 is employed to determine the optical conductivity (σ).

$$\sigma = \frac{\alpha n c}{4\pi} \qquad (5)$$

where σ denotes the optical conductivity (S^{-1}), α represents the absorbance coefficient (cm^{-1}), n signifies the refractive index, and c indicates the speed of light (3×10^{10} cm/s) [34].

When polystyrene is doped with nanometer-scale oxides, the nano-oxides may introduce novel electronic states inside the polymer matrix. This may result in augmented optical responses owing to more excellent charge transfer and photonic characteristics. Incorporating nanoparticles enhances the optical conductivity (σ) of thin films, as demonstrated in Figure (8). The PS/TiO$_2$ sample exhibits the highest optical conductivity compared to the other samples, especially within the wavelength range of 700-950 nm [35, 36].

3.9. Dielectric constant of blank PS, and PS/ nano oxide films

Variations in electrical conductivity are correlated with the number of charges in a material, as indicated by the dielectric constant, which is ascribed to an increase in the mobility of unbound electrons from their orbits. The dielectric constant quantifies the ability of polymeric materials to store charge carriers. Equation 6 identifies two components of the dielectric constant (ε): the actual dielectric constant (ε_r) and the imaginary dielectric constant (ε_i).

$$\varepsilon = \varepsilon_{r(\omega)} + i\, \varepsilon_{i(\omega)} \qquad (6)$$

The dielectric constant parameters are associated with the n and k values, which may be derived from equation 7 [37, 38].

$$\varepsilon_r = n^2 - k^2, \varepsilon_i = 2n\,k \qquad (7)$$

Figures 8 and 9 illustrates the real and imaginary dielectric constants of each sample of plain polystyrene (PS) and PS incorporated with various nano-oxides. The dispersion of the nano-oxide within the PS lattice across all samples is primarily responsible for the actual dielectric constant (ε_r), which is also associated with absorption. This demonstrates that the wavelength is correlated with the actual dielectric constant (ε_r) fluctuation for all samples. Adding nano-oxide to the PS lattice increases ε1, thereby improving dispersion. The ε_r value of the optimal sample, PS/TiO$_2$, is higher than that of the other thin films [39]. Also doping polystyrene with nano-oxides often elevates the imaginary component of the dielectric constant, signifying enhanced energy dissipation attributed to interfacial polarization, dipolar relaxation, and conductive losses.
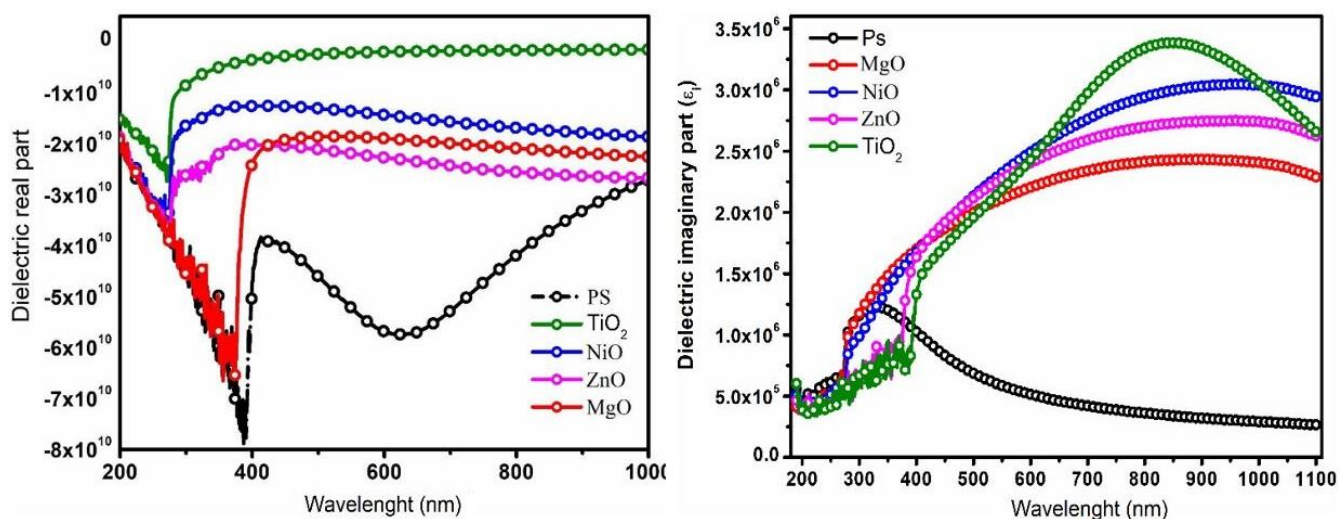

Figure 8: Dielectric real part of blank PS, and PS/ nano oxide films.
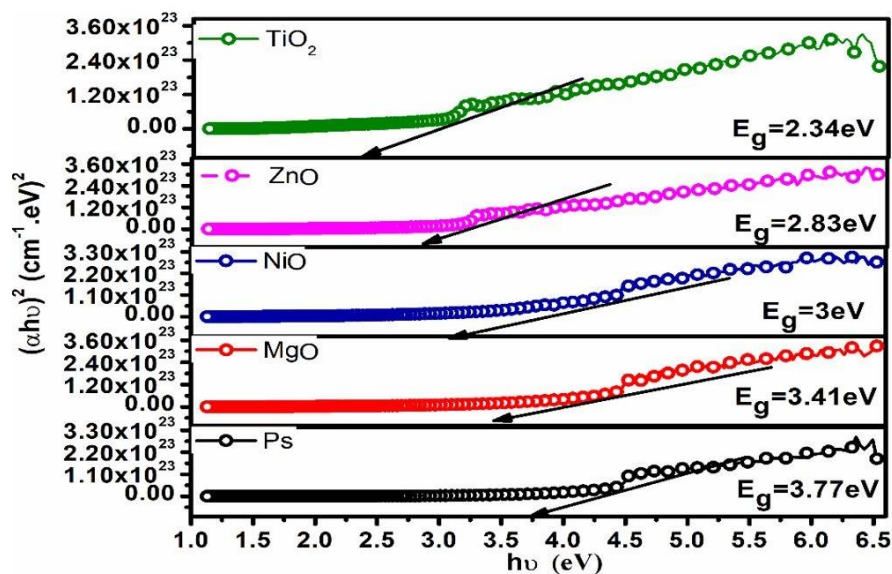
Figure 9: Dielectric imaginary part of blank PS, and PS/ nano oxide films.

3.10. Optical energy gap of blank PS, and PS/nano oxide films

Figure 10 shows the optical energy gap (E_g) is as follows: blank PS (E_g = 3.77 eV), PS/MgO (E_g = 3.41 eV), PS/NiO (E_g = 3.00 eV), PS/ZnO (E_g = 2.83 eV), PS/ TiO_2 (E_g = 2.34 eV). Polystyrene has a substantial energy gap, which imparts exceptional insulating qualities. Doping with nano-oxides may alter its electrical characteristics; yet, in its unadulterated state, polystyrene is a wide-band-gap material appropriate for insulation and optical applications. Doping with nano-

oxides may create energy levels inside the band gap of polystyrene, possibly reducing the effective band gap of the composite and enhancing its responsiveness to optical or electrical stimulation, Energy gap (E_g) computed from the equation 8.

$$\alpha h\nu = B(h\nu - E_g)^n \tag{8}$$

The constant B denotes semiconducting demand, E_g the optical energy gap of the nanocomposite thin film, and n the kind of transition order [40].
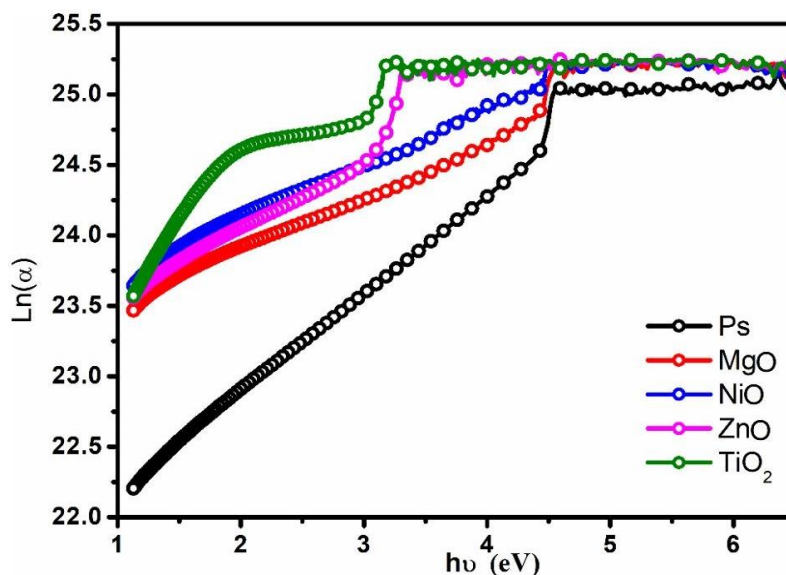

Figure 10: Illustrates the optical energy gap (E_g) as a function of photon energy for both blank PS and PS/ nano oxide films.

3.11. Urbach energy of blank PS, and PS/ nano oxide films

Urbach energy denotes the extent of the tail of localized states inside the band gap, often linked to material disorder. It immediately delineates the exponential absorption edge in the optical absorption spectrum under the fundamental absorption edge (band gap). Urbach energy elucidates the extent of the disorder, flaws, or faults inside a material which doping may affect.

Doping polystyrene with nano-oxides may elevate the Urbach energy, indicating that adding nanoparticles creates more localized states and disorders within the polymer matrix. This alteration is contingent upon several aspects, including the kind of nano-oxide, concentration, dispersion quality, and the interaction between the polymer and the nanoparticles Figure 11, the Urbach energy (Eu) may be calculated from equation 9.

$$\alpha = \alpha_o \exp \frac{h\nu}{E_u} \qquad (9)$$

Where (α_o) denotes a constant, and (Eu) represents Urbach energy. Urbach energy (Eu) is calculated using equation 10 by using the logarithm [41].

$$\ln\alpha = \ln \alpha_o + \frac{h\nu}{E_u} \qquad (10)$$

3.12. Optoelectronic properties of PS and PS nano-oxide thin films

3.12.1. Wemple di-domenico model of PS and PS/nano-oxide thin film

The dispersion energy parameters are essential for designing optoelectronic devices for spectrum dispersion and selecting materials for applications. Therefore, these energy characteristics can be classified as the adequate energy of a singular oscillator (E_0) and dispersion energy (E_d). Consequently, the Single Effective Oscillator Model, which Wemple-Di-Domenico devised, is employed to analyze these attributes. The optical energy gap around the material's band boundaries (valence and conduction) is significantly impacted by the dispersion energy parameters, which diverge from it due to localized states within the bands. This reduces the optical energy gap and significantly affects absorbance. The dielectric constant decrease, denoted by E_d, is associated with modifications in the material's structural arrangement.

As a result, this energy quantifies the average intensity of optical transitions within the band. E_o provides a quantifiable assessment of the material's comprehensive band structure [42]. It is important to note that these energy values may be obtained from equation 11.

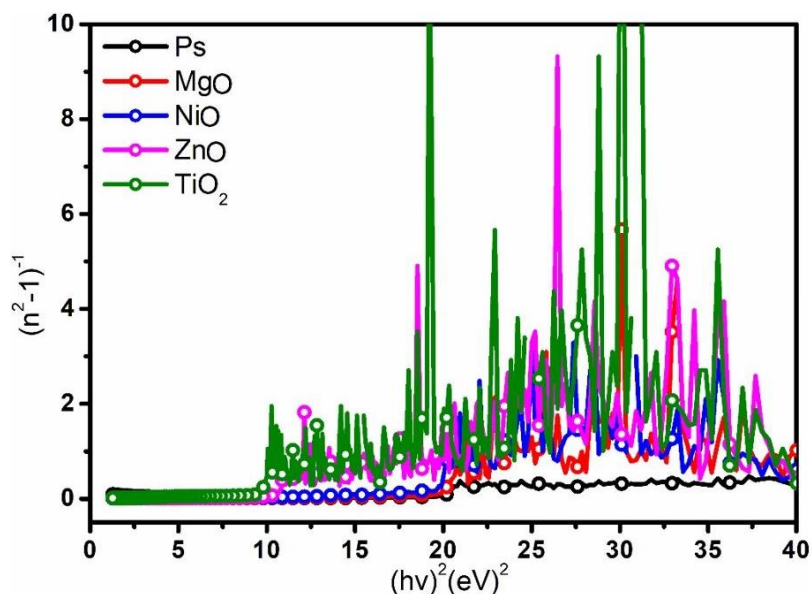$$\left(n^2 - 1\right)^{-1} = \frac{E_0}{E_d} - \frac{(h\nu)^2}{E_d E_o} \qquad (11)$$

Figure 11: Urbach energy gap (E$_g$) for both blank PS and PS/ nano oxide films.

Figure 12 illustrates that the values of Ed and E_o increase with the incorporation of nano-oxide, leading to improved mobility of electrons and holes across the optical energy gap. As a result, the absorption of the nanocomposite thin films is markedly increased, hence reducing the optical energy gap.

3.12.2. Tangent decrease of the dielectric constant in PS nano oxide thin films

When subjected to an alternating electric field, a material's tangent delta (tan δ) measures dielectric loss. This value is crucial for evaluating the energy dissipated as heat inside the material. The tangent loss in polystyrene doped with nano-oxides is considerable owing to these nanoparticles' conductive and dielectric characteristics. The vibration of the PS structure is the consequence of the conversion of photon energy to phonon energy when applied to the particles. The energy lost from electron transitions between orbits and the band gap is quantified by the tangent loss of the dielectric constant (tan δ). The tangent loss (tan δ) is calculated by dividing the imaginary component (ε_i) by the fundamental component (ε_r) of the dielectric constant, as illustrated in equation 12 [43].

$$\tan \delta = \frac{\varepsilon_i}{\varepsilon_r} \tag{12}$$

Where tan δ represents the tangent loss of the dielectric constant.

Figure 13 often demonstrates a rise in tangent loss attributed to heightened interfacial polarization and dielectric losses, particularly at elevated doping concentrations and within certain frequency ranges. The elevated tan δ arises from the interaction between the polymer matrix and the high dielectric constant of the nano-oxides, which improves both (ε_i) and (ε_r), resulting in energy dissipation as heat [44-46].

3.12.3. SELF and VELF of PS / PS nano oxide thin films

The Single Oscillator Energy Loss Function (SELF) and the Valence Electronic Loss Function (VELF) are metrics used to analyze the electronic properties of materials, especially in polymer composites such as polystyrene (PS) infused with nano-oxides. SELF refers to the energy dissipation encountered by an electron during its interaction with a material and is often linked to interbond transitions. VELF delineates energy dissipation attributable to valence electrons and is intricately linked to the material's dielectric characteristics and electron density (Figures 14 and 15).
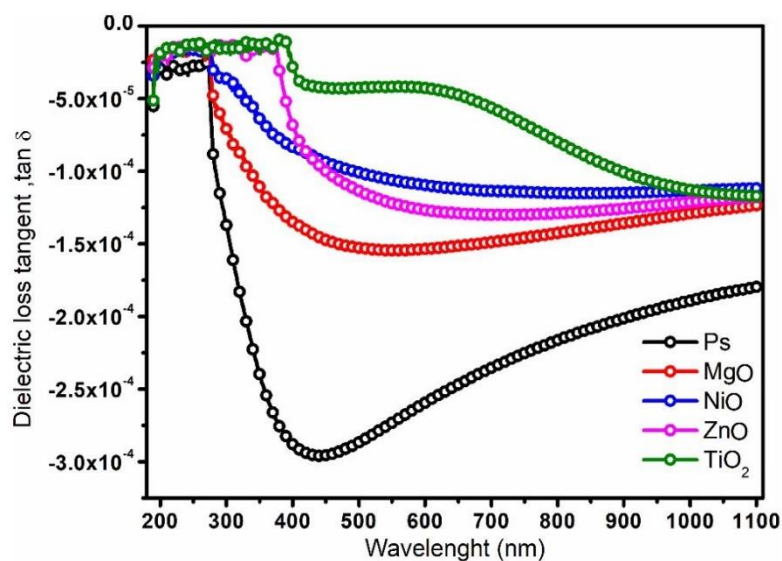

Figure 12: $(n^2 - 1)^{-1}$ comparison of variation against $(h\nu)^2$ for the blank PS, and PS/ nano oxide thin films.
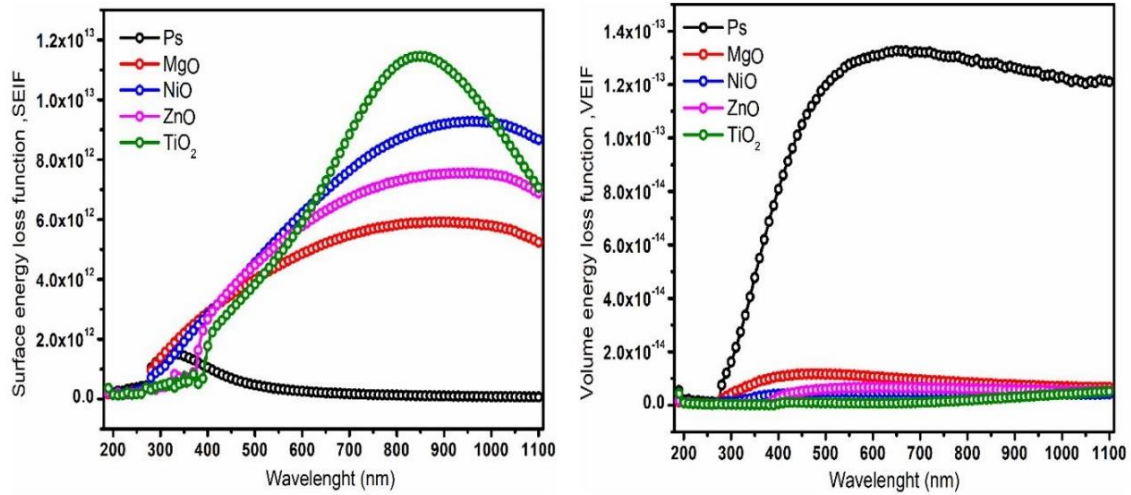
Figure 13: Dielectric constant tangent loss for the blank PS, and PS/ nano oxide films.

Doping PS with nano-oxides affects both SELF and VELF because of the increased permittivity and electron interactions induced by the oxide nanoparticles. These functions elucidate the changes in dielectric characteristics inside PS composites, offering insights into applications such as energy storage, sensors, and shielding materials, where electronic qualities are crucial. The equations 14 and 15 facilitate the calculation of surface and volume losses, which are directly related to the real (ε_r) and imaginary (ε_i) components of the dielectric constant [47].

$$\left[VELF = \frac{\varepsilon_i}{\varepsilon_r^2 + \varepsilon_i^2} \right] \tag{13}$$

and

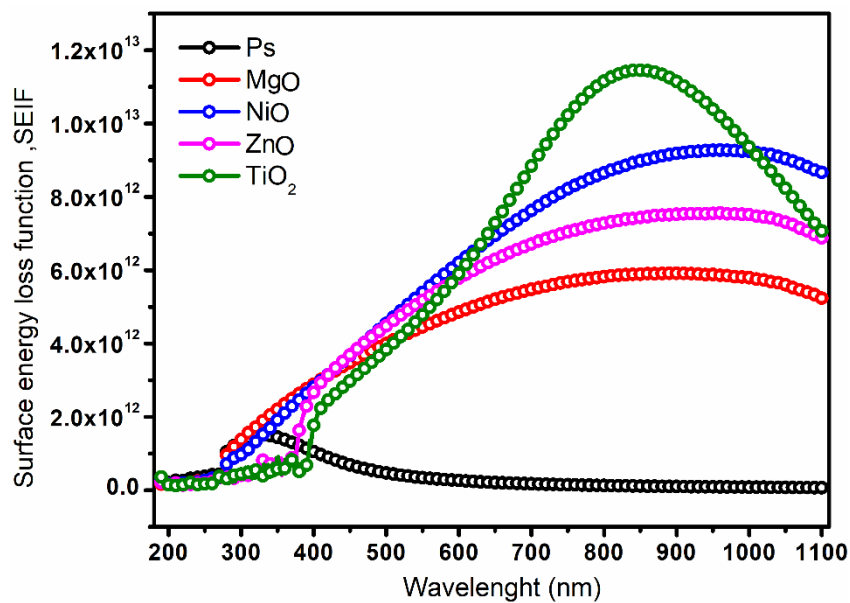$$\left[SELF = \frac{\varepsilon_i}{((\varepsilon_r + 1)^2 + \varepsilon_i^2)} \right] \tag{14}$$

Figure 14: Fluctuations in SELF as a function of wavelength for both the blank PS and the PS/nano oxide films.
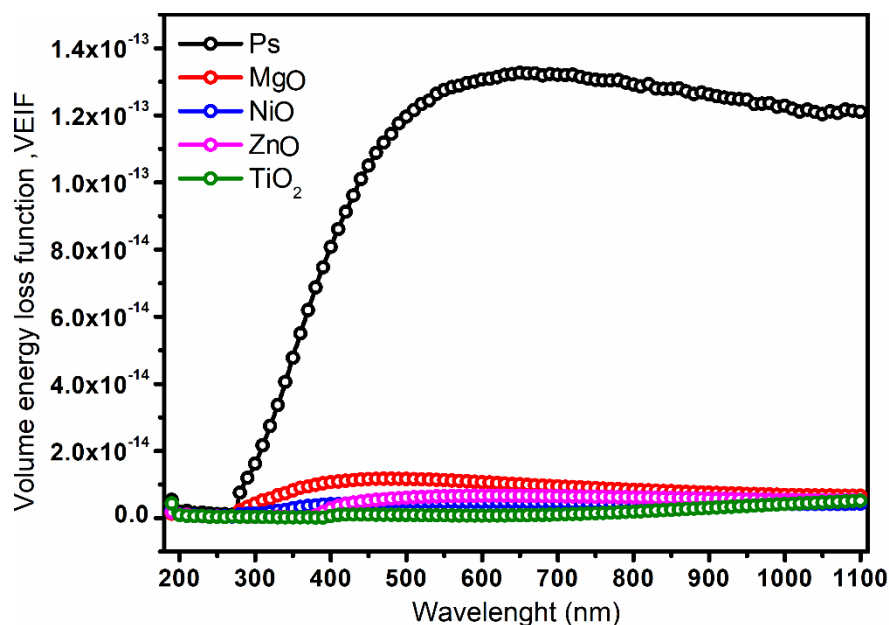
Figure 15: Fluctuations in VELF as a function of wavelength for both the blank PS and the PS/nano oxide films.

3.13. FESEM of PS thin films

0.01 g of nanoparticles, including ZnO, NiO, MgO, and TiO$_2$, were amalgamated with a PS lattice to fabricate the nanocomposite thin films. The nanoparticles were successfully disseminated inside the lattice-structured PS, Figure 16. The inspection with FESEM is shown. The unembellished PS thin film often displays a polished surface. Conversely, the surface of polystyrene displays heightened granularity or roughness attributable to the inclusion of nano-oxide particles [48, 49]. Scanning electron microscope images showed that the nanoparticles are (23.19, 40.93, 31.13, 46.90, 47.43) for PS, ZnO, TiO$_2$, MgO, and NiO respectively.

3.14. AFM examination of PS and PS/nano oxides thin film

The atomic force microscope (AFM) obtained the surface topography of the uncoated polystyrene (PS) and PS/nano-oxide thin films. Each shot depicts morphological evaluations of the surface, including average surface roughness, root mean square, surface area, and surface kurtosis. The photos indicate that the roughness of the PS/nano-oxides thin films is much superior to that of the blank PS Figure 17. Moreover, the integration of nanoparticles increases the roughness of the PS matrix, an essential factor for absorption (Table 1) [50, 51].

Table 1: Roughness Sg, mean roughness Sa, and maximum height.

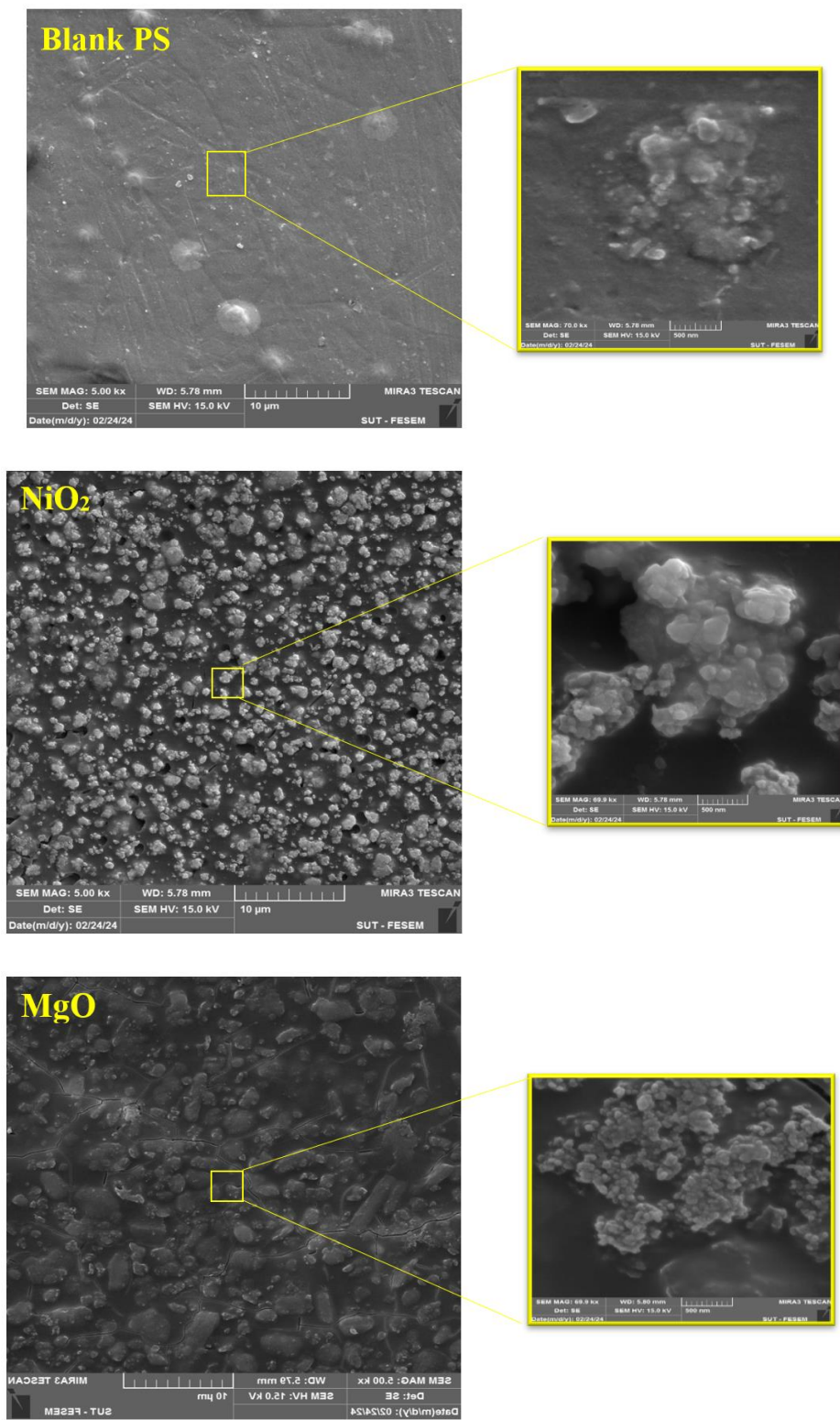| Sample	RMS roughness (Sq); nm	Mean roughness (Sa); nm	Maximum Height (Sz); nm
PS	5.137	3.5	74.8
NiO$_2$	5.239	3.6	70.52
MgO	7.33	4.9	74.2
TiO$_2$	4.125	3.09	45.41
ZnO	6.83	4.8	79.4

Figure 16: FESEM pictures for the blank PS and PS/ nano oxide films after 300h irradiation.
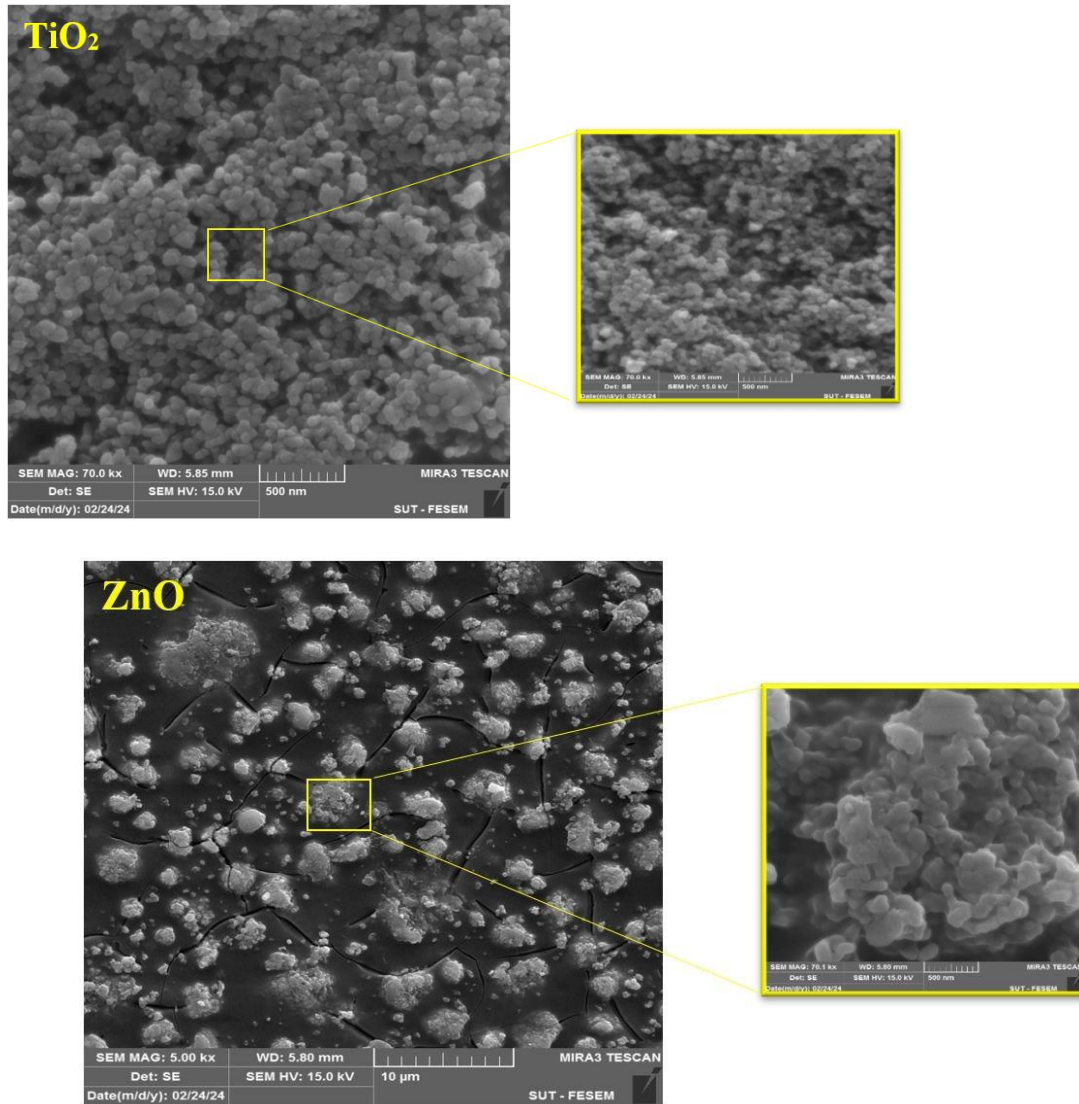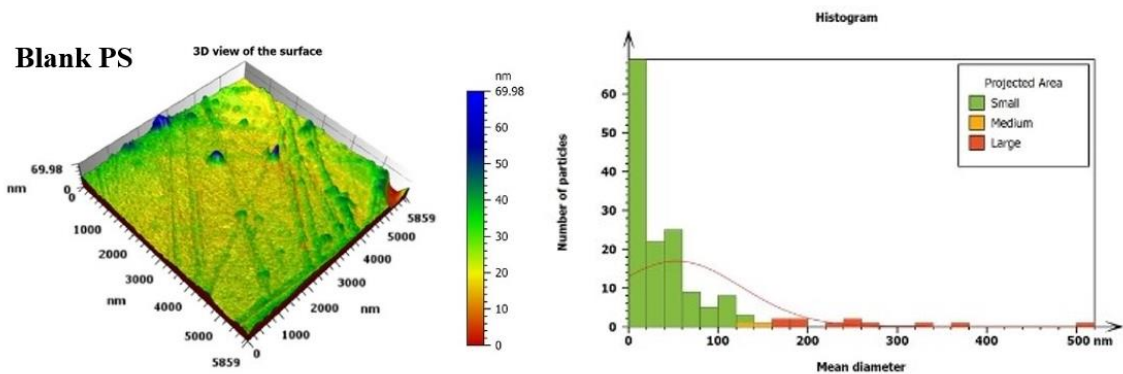
Figure 16: Continue.

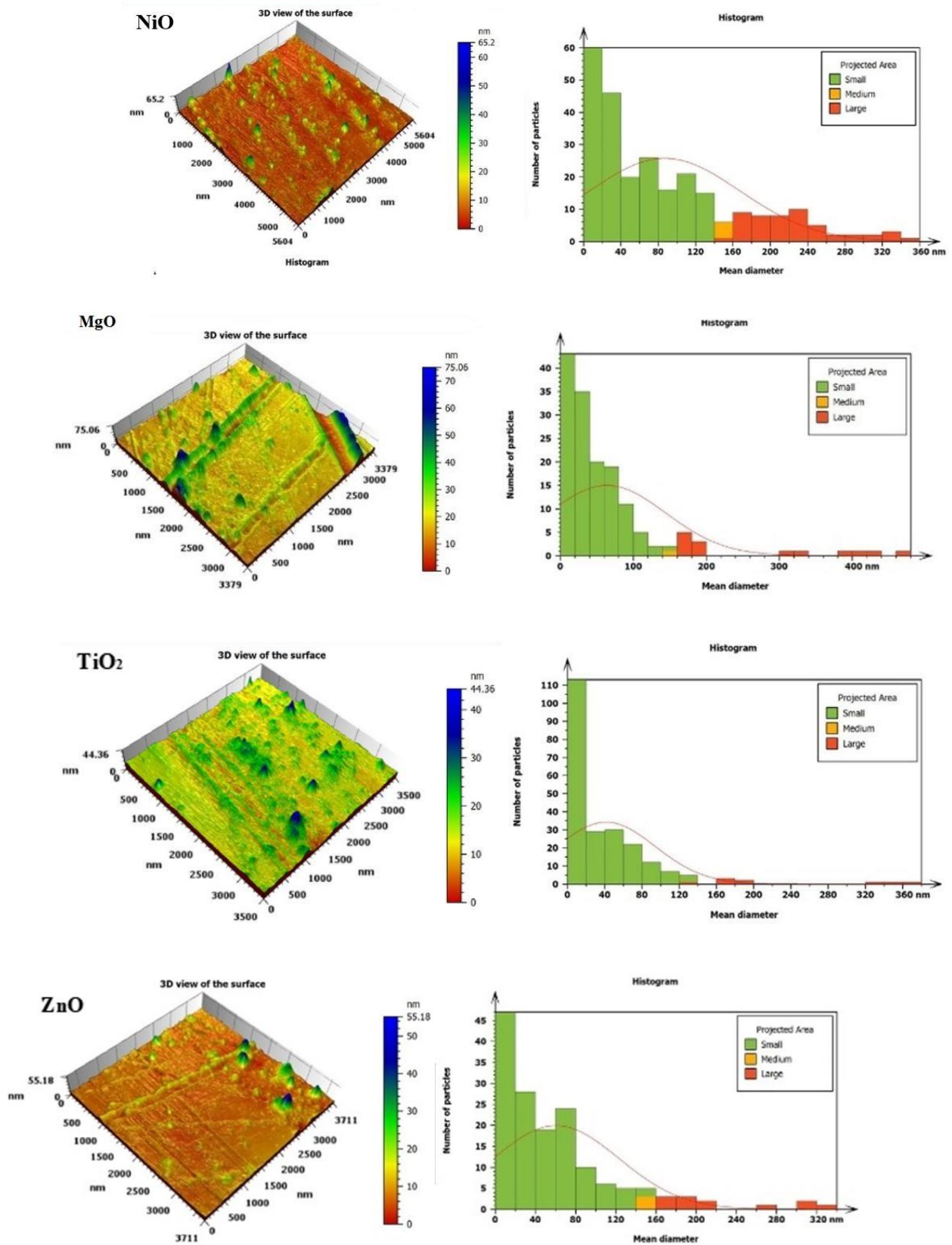**Figure 17:** AFM pictures for the blank PS and PS/ nano oxide films.

Figure 17: Continue.

4. Conclusion

The research effectively produced polystyrene (PS) nanocomposite polymer thin films doping with metal oxide nanoparticles, such as ZnO, TiO$_2$, NiO, and MgO, by a casting method. The incorporation of these nanoparticles markedly altered the optical energy gap of the PS matrix, improving light absorption in both the ultraviolet and visible wavelengths. This integration enhanced the optoelectronic characteristics, yielding increased dielectric constants at higher frequencies and a diminished effective mass. The findings indicated substantial enhancements in reflectance, transmittance, and high-frequency dielectric characteristics, accompanied by a decreased optical bandgap and improved UV stability. These results validate the materials' appropriateness for applications including UV protection, LEDs, laser sensors, and energy conversion devices. The enhancements render these materials suitable for sophisticated optoelectronic applications, providing improved photostability and weather resistance, thereby making them optimal for usage such as UV shielding, light-emitting diodes, laser sensors, memory devices, and potentially solar cells. The results indicate intriguing avenues for further research, especially in optimising doping doses and investigating diverse nanoparticles to create composite materials with enhanced performance in energy, communications, and sensing applications.

Acknowledgements

5. References

1. Gaabour LH. Effect of addition of TiO$_2$ nanoparticles on structural and dielectric properties of polystyrene/polyvinyl chloride polymer blend. AIP Adv. 2021;11(10):1-9. https://doi.org/10.1063/5. 0062445.

2. Alam MA, Arif S, Shariq M. Enhancement in mechanical properties of polystyrene-ZnO nanocomposites. Int J Innov Res Adv Eng. 2015; 6(2): 122-9.

3. Almara R, Huseynova A, Musayeva N. Comprehensive analysis of ZnO-doped polystyrene nanocomposites: structural, optical and defect analysis. J Thermoplast Compos Mater. 2024. https://doi.org/10.1177/08927057241291794.

4. Iulianelli GCV, David GDS, dos Santos TN, Sebastião PJO, Tavares MIB. Influence of TiO$_2$ nanoparticle on the thermal, morphological and molecular characteristics of PHB matrix. Polym Test. 2018; 65:156-62.

5. Cazan C, Enesca A, Andronic L. Synergic effect of TiO$_2$ filler on the mechanical properties of polymer nanocomposites. Polymers (Basel). 2021;13(12):2017. https://doi.org/10.3390/polym13122017

6. Khodair ZT, Ibrahim NM, Kadhim TJ, Mohammad AM. Synthesis and characterization of nickel oxide (NiO) nanoparticles using an environmentally friendly method, and their biomedical applications. Chem Phys Lett. 2022; 797:139564. https://doi.org/10.1016/ j. cplett.2022.139564

7. Giorgio G, Maddalena P. Optical Properties of Materials. 2005;183-91. https://doi.org/10.1016/B978-0-12-803581-8.01184-X.

8. Jebur QM, Hashim A, Habeeb MA. Structural, electrical and optical properties for (polyvinyl alcohol–polyethylene oxide–magnesium oxide) nanocomposites for optoelectronics applications. Trans Electr Electron Mater. 2019;20(4):334-43. https://doi.org/10.1007/s42341-019-00121-x

9. Abdel-Kader MH, Alhazime AA, Mohamed MB. Tailoring the optical properties (linear and nonlinear) of triple-blended polymers via reinforcement of mixed (SnO$_2$ and NiO) nanofillers for promising applications. Opt Quantum Electron. 2023;55(11): 1029. https://doi.org/10.1007/s11082-023-05266-x

10. Kumar V, Ayoub I, Sharma V, Swart HC, editors. Optical properties of metal oxide nanostructures. Berlin: Springer; 2023.

11. Alsaad AM, Al-Bataineh QM, Ahmad AA, Jum'h I, Alaqtash N, Bani-Salameh AA. Optical properties of transparent PMMA-PS/ZnO NPs polymeric nanocomposite films: UV-shielding applications. Mater Res Express. 2020;6(12):126446. https://doi.org/10. 1088/ 2053-1591/ab68a0.

12. Ahmed DS, Mohammed A, Husain AA, El-Hiti GA, Kadhom M, Kariuki BM, et al. Fabrication of highly photostable polystyrene films embedded with organometallic complexes. Polymers. 2022;14(5): 1024. https://doi.org/10.3390/polym14051024.

13. Baysal T, Noor N, Demir A. Nanofibrous MgO composites: structures, properties, and applications. Polym Plast Technol Mater. 2020; 59(14):1522-51. https://doi.org/10.1080/25740881.2020.1759212.

14. Sharma A, Karthikeyan B. Optical and sign-flipping nonlinear optical properties of NiO/PMMA/PANI nanocomposite films. Opt Mater. 2024;116297. https://doi.org/10.1016/j.optmat.2024.116297.

15. Nguyen TV, Dao PH, Duong KL, Duong QH, Vu QT, Nguyen AH, et al. Effect of R-TiO$_2$ and ZnO nanoparticles on the UV-shielding efficiency of water-

borne acrylic coating. Prog Org Coat. 2017; 110:114-21. https://doi.org/10.1016/j.porgcoat.2017.02.017.

16. Dolai S, Sarangi SN, Hussain S, Bhar R, Pal AK. Magnetic properties of nanocrystalline nickel incorporated CuO thin films. J Magn Magn Mater. 2019; 479:59-66. https://doi.org/10.1016/j.jmmm.2019.02.005

17. Al-Mahweet Y. Physicochemical properties of prepared ZnO/polystyrene nanocomposites: structure, mechanical and optical. J Ovonic Res. 2020;16(1):71–81.

18. Pepe Y, Karatay A, Donar YO, Yildiz EA, Sınağ A, Unver H, Elmali A. Enhanced nonlinear absorption coefficient and low optical limiting threshold of NiO nanocomposite films. Optik. 2021; 227:165975. https://doi.org/10.1016/j.ijleo.2020.165975.

19. Zeinali M, Jaleh B, Vaziri MR, Omidvar A. Study of nonlinear optical properties of TiO₂–polystyrene nanocomposite films. Quantum Electron. 2019; 49(10):951. https://doi.org/10.1070/QEL16923.

20. Tu Y, Zhou L, Jin YZ, Gao C, Ye ZZ, Yang YF, et al. Transparent and flexible thin films of ZnO-polystyrene nanocomposite for UV-shielding applications. J Mater Chem. 2010; 20(8):1594-9. https://doi.org/10.1039/B914156A.

21. Dong L. Optical properties of nanoparticles in composite materials [dissertation]. Stockholm: KTH Royal Institute of Technology; 2012.

22. Olson E, Li Y, Lin FY, Miller A, Liu F, Tsyrenova A, et al. Thin biobased transparent UV-blocking coating enabled by nanoparticle self-assembly. ACS Appl Mater Interfaces. 2019; 11(27):24552-9. https://doi.org/10.1021/acsami.9b05383

23. Sharma T, Garg M. Polystyrene/ZnO nanocomposite films with optimized optical properties for UV-shielding applications. Trans Electr Electron Mater. 2023; 24(3):217-27. https://doi.org/10.1007/s42341-023-00437-9.

24. Hassanien AS, Akl AA. Influence of composition on optical and dispersion parameters of thermally evaporated non-crystalline Cd50S50− xSex thin films. J Alloys Compd. 2015; 648:280-90. https://doi.org/10.1016/j.jallcom.2015.06.231.

25. Ji L, Liu L, Li H, Ji Y. The molecular design and characterization of a transparent and flexible TiO₂/polymer nanocomposite with antibacterial and anti-UV light properties. J Polym Res. 2023;30(4):149. https://doi.org/10.1007/s10965-023-03530-y.

26. Kudryashov A, Baryshnikova S, Gusev S, Tatarskiy D, Lukichev I, Agareva N, et al. UV-induced gold nanoparticle growth in polystyrene matrix with soluble precursor. Photonics. 2022;9(10):776. https://doi.org/10.3390/photonics9100776.

27. Ritchie AW, Cox HJ, Gonabadi HI, Bull SJ, Badyal JPS. Tunable high refractive index polymer hybrid and polymer–inorganic nanocomposite coatings. ACS Appl Mater Interfaces. 2021;13(28):33477-84. https://doi.org/10.1021/acsami.1c08612.

28. Cheng Y, Lu C, Yang B. A review on high refractive index nanocomposites for optical applications. Recent Pat Mater Sci. 2011;4(1):15-27. https://doi.org/10.2174/1874464811104010015.

29. Hassanien AS, Akl AA. Optical characteristics of iron oxide thin films prepared by spray pyrolysis technique at different substrate temperatures. Appl Phys A. 2018;124(11):752. https://doi.org/10.1007/s00339-018-2130-0.

30. Yang C, Fan H, Xi Y, Chen J, Li Z. Effects of depositing temperatures on structure and optical properties of TiO₂ film deposited by ion beam assisted electron beam evaporation. Appl Surf Sci. 2008;254(9):2685-9. https://doi.org/10.1016/j.apsusc.2007.10.034.

31. Al-Bataineh QM, Alsaad AM, Ahmad AA, Al-Sawalmih A. Structural, electronic and optical characterization of ZnO thin film-seeded platforms for ZnO nanostructures: sol–gel method versus ab initio calculations. J Electron Mater. 2019; 48:5028-38. https://doi.org/10.1007/s11664-019-07245-0.

32. Loste J, Lopez-Cuesta JM, Billon L, Garay H, Save M. Transparent polymer nanocomposites: an overview on their synthesis and advanced properties. Prog Polym Sci. 2019; 89:133-58. https://doi.org/10.1016/j.progpolymsci.2018.10.001.

33. Zare Y, Shabani I. Polymer/metal nanocomposites for biomedical applications. Mater Sci Eng C. 2016; 60:195-203. https://doi.org/10.1016/j.msec.2015.11.023

34. Hewa-Rahinduwage CC, Jayasuriya AC. Polymer nanocomposites with ZnO nanoparticles for bone tissue engineering. Polym Plast Technol Eng. 2020; 59(12):1362-76. https://doi.org/10.1080/03602559.2020.1785790.

35. Horst A, Amberg-Schwab S, Organisch-M, Schroers H. Properties and applications of highly transparent glass coatings for UV protection and light management. Thin Solid Films. 2023; 561:10903–18.

36. Kusior K, Jaworski A, Mazur M. Deposition and morphology of thin composite coatings for optical purposes. Appl Phys A. 2018;124(4):186. https://doi.org/10.1007/s00339-018-1670-0.

37. Hoffmann SC, Hildgen P. Synthesis of ZnO-filled polystyrene for optical electronics. Opt Mater. 2014; 46:25-31. https://doi.org/10.1016/j.optmat.2014.03.021.

38. Takai C, Osawa M, Kawai T. Polymer dispersed hybrid optics: Design methods. J Alloys Compd. 2021; 854:15593–9.

39. Basak U, George BP. Zinc-based nano hybrids for anti-bacterial multilayer films. Prog Polym Sci. 2020; 104:20015–34.

40. Nisar S, Iqbal R, Latif N. Titanium-doped nanocoating: engineering brilliance. Optics Express. 2019;28(10):15091–107. https://doi.org/10.1016/10.1364/OE.384905

41. Zayed F. Simplified suspension spraying technology. J Mater Sci Mater Electron. 2022; 30(17):15254-60.

42. Yılmaz M, Koltsov AE. Enhanced light-blocking

material studies. Mater Today. 2013;16(5):168-72.

43. Sharma T, Garg M. Polystyrene/ZnO nanocomposite films with optimized optical properties for UV-shielding applications. Trans Electr Electron Mater. 2023;24(3):217-27. https://doi.org/10.1016/10. 1007/ s42341-023-00437-9

44. Hassanien AS, Akl AA. Influence of composition on optical and dispersion parameters of thermally evaporated non-crystalline Cd50S50−xSex thin films. J Alloys Compd. 2015; 648:280-90. https://doi.org/10. 1016/j.jallcom.2015.06.231.

45. Ji L, Liu L, Li H, Ji Y. The molecular design and characterization of a transparent and flexible TiO2/polymer nanocomposite with antibacterial and anti-UV light properties. J Polym Res. 2023; 30(4):149. https://doi.org/10.1016/10.1007/ s10965-023-03147-0.

46. Kudryashov A, Baryshnikova S, Gusev S, Tatarskiy D, Lukichev I, Agareva N, et al. UV-induced gold nanoparticle growth in polystyrene matrix with soluble precursor. Photonics. 2022;9 (10):776. https://doi.org/10.1016/10.3390/photonics9100776.

47. Ritchie AW, Cox HJ, Gonabadi HI, Bull SJ, Badyal JPS. Tunable high refractive index polymer hybrid and polymer–inorganic nanocomposite coatings. ACS Appl Mater Interfaces. 2021;13(28):33477-84. https://doi.org/10.1016/10.1021/acsami.1c08656.

48. Cheng Y, Lu C, Yang B. A review on high refractive index nanocomposites for optical applications. Recent Pat Mater Sci. 2011; 4(1):15-27. https://doi.org/ 10.1016/10.2174/2212797711795049017.

49. Hassanien AS, Akl AA. Optical characteristics of iron oxide thin films prepared by spray pyrolysis technique at different substrate temperatures. Appl Phys A. 2018; 124(11):752. https://doi.org/ 10. 1016/ 10.1007/s00339-018-2121-0.

50. Yang C, Fan H, Xi Y, Chen J, Li Z. Effects of depositing temperatures on structure and optical properties of TiO2 film deposited by ion beam assisted electron beam evaporation. Appl Surf Sci. 2008; 254 (9):2685-9. https://doi.org/10.1016/10.1016/j. apsusc. 2007.10.029

51. Al-Bataineh QM, Alsaad AM, Ahmad AA, Al-Sawalmih A. Structural, electronic, and optical characterization of ZnO thin film-seeded platforms for ZnO nanostructures: sol–gel method versus ab initio calculations. J Electron Mater. 2019; 48:5028-38. https://doi.org/10.1016/10.1007/s11664-019-07347-2